Journal of Cleaner Production 327 (2021) 129432

Contents lists available at ScienceDirect

Journal of Cleaner Production

journal homepage: www.elsevier.com/locate/jclepro

Enhancing Biobutanol Production from biomass willow by pre-removal of water extracts or bark

Jinze Dou [a,*], Vijaya Chandgude [a], Tapani Vuorinen [a,**], Sandip Bankar [a], Sami Hietala [b], Huy Quang Lê [a]

[a] Department of Bioproducts and Biosystems, Aalto University, Espoo, Finland
[b] Department of Chemistry, University of Helsinki, Helsinki, Finland

ARTICLE INFO

Handling Editor: Cecilia Maria Villas Bôas de Almeida

Keywords:
Biobutanol
Debarking
Phenol aldehyde condensate
Water extracts
Willow bark

ABSTRACT

Aiming to understand the importance of debarking on the controlled utilization of phenolic-rich willow biomass, biobutanol was produced from it by using *Clostridium acetobutylicum*. Acid-catalysed steam explosion and enzymatic hydrolysis (EH) were investigated before the acetone-butanol-ethanol (ABE) fermentation. The hydrolysable sugar yield and ABE fermentation efficiency were found to decline progressively from willow wood (WW) to HWE WB (hot water extracted willow biomass), WB (willow biomass) and the WW + HWE (willow wood plus the artificial willow bark water extracts), indicating that the pre-removal of water extracts or the bark can significantly improve ABE yield. Notably, the ABE productivity of WW achieved 12.7 g/L at the solvent yield of 31%, and the butanol concentration (i.e. 8.5 g/L) generated by WW is relatively high among the reported lignocellulosic-derived biomass. Additionally, it is hypothesized that under acidic conditions and high temperatures the fructose present in willow water extracts form hydroxymethylfurfural during steam explosion, which then spontaneously condenses with phenolic substances of willow bark to form a solid furanic precipitate. The formed furanic precipitates play inhibitory role in the enzymatic hydrolysis and are thereby deleterious to the ABE fermentation.

1. Introduction

Clean energy alternatives are of prime importance because of detrimental environmental impacts caused by conventional fossil fuels. Therefore, the renewable energy and chemicals production is getting attention in the light of increasing global demand, to replace the traditional petroleum-based fuels. Naturally photosynthesized lignocellulosic biomass is seen as promising, predictable, and sustainable source of carbon to satisfy such demand (Isikgor and Becer, 2015). Biofuels, for instance the small chain alcohols (ethanol and methanol) and long chain alcohols (*n*-butanol), can be biologically generated from lignocellulosic-derived biomass (Birgen et al., 2019; Jørgensen et al., 2007). Butanol stands out from the ethanol in many characteristics, such as its higher calorific value due to its longer carbon chain, lower volatility and corrosivity (Bankar et al., 2013), and higher compatibility to the current diesel engine (da Silva Trindade and dos Santos, 2017) which has high resemblance to gasoline.

Lignocellulose is mainly composed of cellulose, hemicellulose, lignin, and extractives. Cellulose, the most abundant polymer in the world, is constituted by the repeated glucose units that are bonded by *β*-(1,4)-glycosidic linkages (French, 2017), which can be enzymatically depolymerized into its fermentable monomeric sugars (Jørgensen et al., 2007). Hemicelluloses act as the link between lignin and cellulosic components in the cell wall. The primary hemicellulose in hardwood is glucuronoxylan, containing xylose and glucuronic acid as the main constituents. It is a linear polymer composed of *β-D*-xylopyranosyl units linked by β-(1,4)-glycosidic bonds and substituted by 4-O-methyl-D-glucopyranosyluronic acid and acetyl groups. Therefore, acetic acid is generated under the autohydrolysis pre-treatment (e.g. steam explosion). Additionally, the 5-hydroxymethyl furfural (HMF) and furfural (Steinbach et al., 2017; Choudhary et al., 2012) can be formed under the dehydration of hexose and pentose mono sugars, respectively. Aldehydes (e.g. HMF and furfural) and phenols can condense, forming condensed precipitate (Koch and Pein, 1985). Lignin, another

* Corresponding author.
** Corresponding author.
E-mail addresses: jinze.dou@aalto.fi (J. Dou), tapani.vuorinen@aalto.fi (T. Vuorinen).

https://doi.org/10.1016/j.jclepro.2021.129432
Received 26 July 2021; Received in revised form 10 October 2021; Accepted 19 October 2021
Available online 22 October 2021

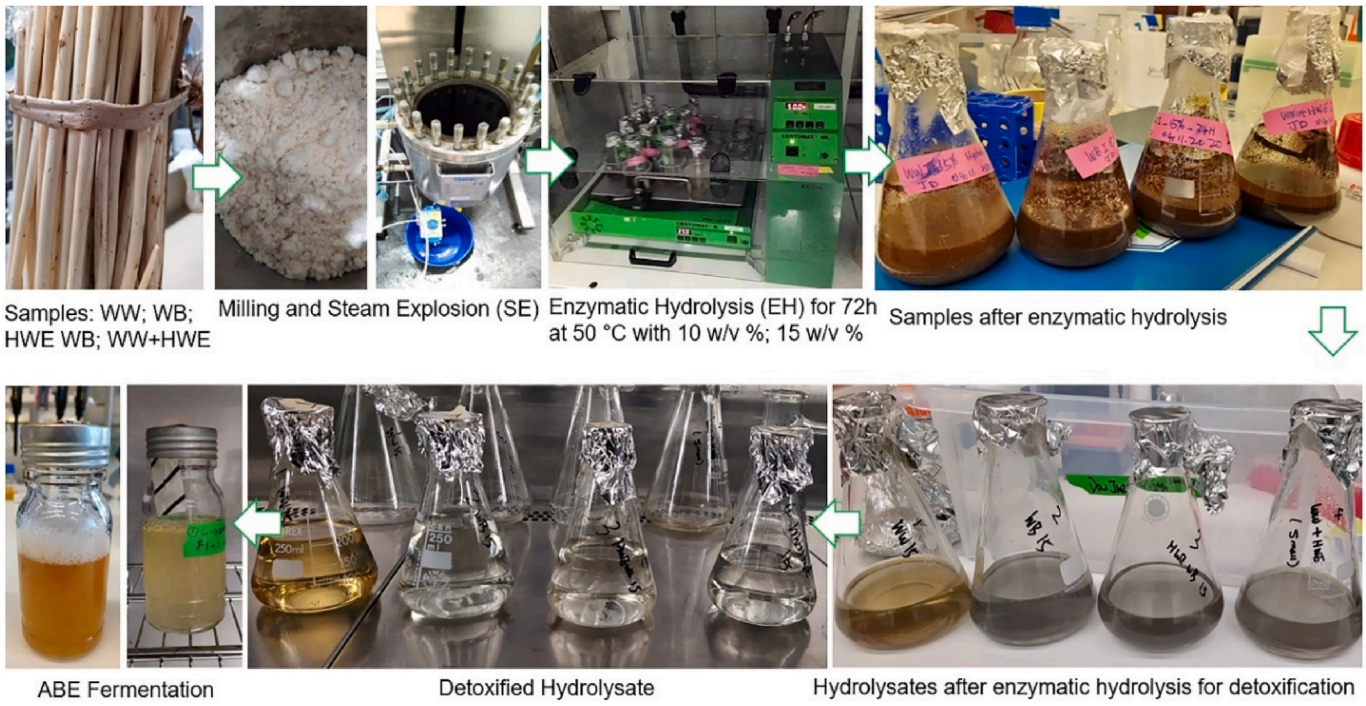

Fig. 1. Experimental protocol of enzymatic hydrolysis and fermentation after the pre-treatment of steam explosion: WW = willow wood; WB = willow biomass (including bark); HWE WB = hot water extracted willow biomass; WW + HWE = willow wood + artificial Klara Bark water extracts (21 wt% WW).

amorphous polymer, is composed mainly of three phenylpropanoid units, that is *p*-hydroxyphenol (H), guaiacyl (G) and syringyl (S) units. Its interunit linkages are *β-O-4* (β-aryl-ether), *β-5* (phenylcoumaran), *β-β* (resinol), *5-5* (biphenyl), and *4-O-5* (biaryl ether) (Dou et al., 2018a). Extractives, rich in bioactive phenolic compounds and monosaccharides, exhibit high occurrence in the bark of trees, such as spruce (Kemppainen et al., 2014), willow (Dou et al., 2018b) and eucalyptus (Dou et al., 2021a).

Pre-treatments, such as steam explosion, are known to bring easier cellulase accessibility by loosening the heterogeneous cell wall of plants and increasing the accessibility of cellulose (Silveira et al., 2015). However, inhibitors for microbial fermentation can be formed during the pre-treatment (Maiti et al., 2016), such as heterocyclic furan derivatives (furfural and HMF), aliphatic acids (formic acid, acetic acid, and levulinic acid) and phenolic aromatic products (ferulic acid, syringaldehyde, and vanillin) from the secondary degradation of lignin. Additionally, enzymatic hydrolysis (Jørgensen et al., 2007) degrades the polysaccharides (cellulose and hemicellulose) into fermentable sugar monomers. *Clostridium* spp. are traditionally known as the anaerobic and fermentative microorganism to produce the butanol from starch rich feedstocks via conventional acetone-butanol-ethanol (ABE) fermentation (Nilsson et al., 2020). The ABE fermentation consists of two major stages (Bankar et al., 2013): 1) acidogenic phase during the exponential growth; 2) solventogenic phase at the end of its exponential growth. Acids (such as acetic acid and butyric acid) are produced during the acidogenic phase as the main products besides gases such as carbon dioxide and hydrogen. The ABE solvents are generated during the solventogenic phase as a metabolic response to the accumulated acids (Bankar et al., 2013). Low yields and productivities of ABE process remains the major limiting factor for its commercial scale operation. Improving the enzymatic hydrolysis efficiency (e.g. grafting the surfactants or the hemicellulose-degrading enzymes) (Eriksson et al., 2002; Zhang et al., 2011), enhancing the metabolic efficiency (e.g. using reducing agents) (Chandgude et al., 2021), elimination of unwanted inhibitors (e.g. detoxification by activated carbons) (Zhang et al., 2018) and enriching the nutrient medium supplementation (e.g. using starchy slurry) (Yang et al., 2017) have been reported to enhance the ABE fermentation.

Planting short-rotation woody crops (SRWC) is one way of supplying lignocellulosic biomass in a sustainable and effective manner. Cultivated willow is an energy crop that grows effectively even at abandoned peatlands with limited fertilization support. For well-managed willow plantations at peatland, the annual productivity can be > 12.3 oven-dry tonnes/ha, which exceeds with about 8–30% the productivity gained with natural forest species (i.e. birch and grey alder) on the same land (Hytönen and Saarsalmi, 2009). In Finland alone, there is approximately 50,000 ha of abandoned peatland non-vegetated forever unless taking active measures. Restoration of such cut-away peatland can mitigate global greenhouse emissions as the mechanical harvesting of peat destroys the original mire ecosystem (Hytönen and Saarsalmi, 2009). Afforestation or peatland rehabilitation by planting the SRWC is a critical step for preventing further peatland degradation.

The controlled deconstruction of willow biomass is proposed for the energy and material uses of willow by debarking it first to wood and bark (Dou et al., 2016). The bark contains a wide array of bioactive metabolites (Dou et al., 2018b) having potential to be further chromatographically purified (Dou et al., 2021b) for high-end pharmaceutical applications (Kesari et al., 2020). The wood fraction could be further valorised to produce fermentable sugars and uses in, e.g., biobutanol generation through ABE fermentation. The objective of this study is first to demonstrate the importance of debarking or recovery of phenolic-rich extractives prior to the controlled use of the remaining wood towards fermentable sugars for further biobutanol production. Secondly, the aim is to clarify how the formation of the highly insoluble polymeric material, phenol-aldehyde condensate, takes place and whether it hinders the biobutanol yield. To do this, the chemical structure of the components is thoroughly investigated.

2. Material & methods

Two-year old "Klara'' hybrid (SalixEnergi Europa AB) (Lindegaard et al., 2011) willow stems were harvested from the field of Carbons Finland Oy in Kouvola, Finland on May 7th, 2019. The bark was manually stripped off from the willow stems to prepare the willow wood

Table 1
Overall chemical composition (%) of the studied samples before and after steam explosion pre-treatment and the enzymatic hydrolysis (10 wt% w/v; 15 wt% w/v) along with respective removal percent. Equation removal = (IA – (SRY * AT))/IA (2); IA refers to the initial amount before the treatment and SRY stands for the solid recovery yield and AT refers to the amount after the treatment. The amount (%) of each component on the original biomass are given in brackets. Standard deviations are given at Table S5. 1.11 and 1.14 are the stoichiometric factors (Pratto et al., 2020) of glucose to equivalent cellulose and xylose to equivalent hemicellulose, respectively.

			Steam explosion (SE) pre-treatment		Enzymatic hydrolysis (EH), 10% w/v		Enzymatic hydrolysis (EH), 15% w/v	
	Component (wt%)	original	After SE	Removal after SE	After EH	Removal after EH/SE (original)	After EH	Removal after EH/SE (original)
WW	equivalent cellulose	41.1	64.0	34.3	44.5	64.0 (76.4)	43.5	61.4 (74.7)
	equivalent hemicellulose	13.5	0.8	97.6	0.6	58.6 (99.0)	0.5	60.6 (99.1)
	Klason lignin	21.0	22.6	54.6	44.0	0 (54.3)	42.1	0 (51.9)
	Extracts	1.9	1.1	76.4	1.4	0 (84.0)	2.1	0 (73.5)
	Ash	0.2	0.1	82.8	0.6	0 (23.6)	0.1	0 (91.9)
	Solid recovery (SRY, %)	–	42.2	–	51.71	–	56.81	–
WB	equivalent cellulose	37.0	53.6	34.7	45.9	36.2 (58.3)	44.8	36.7 (58.7)
	equivalent hemicellulose	11.3	0.7	97.1	0.5	49.1 (98.5)	0.6	35.9 (98.1)
	Klason lignin	25.9	36.1	37.1	47.3	0 (38.7)	43.2	0 (43.1)
	Extracts	2.9	1.17	81.8	1.4	0 (83.8)	1.4	0 (83.3)
	Ash	1.1	0.3	87.1	0.4	0 (88.1)	0.2	0 (94.1)
	Solid recovery (SRY, %)	–	45.0	–	74.53	–	75.73	–
HWEWB	equivalent cellulose	38.1	55.1	27.3	40.5	50.0 (63.7)	43.1	44.7 (59.8)
	equivalent hemicellulose	12.0	0.9	96.2	0.6	55.5 (98.3)	0.7	48.7 (98.0)
	Klason lignin	25.4	34.2	32.3	46.4	0 (37.5)	43.1	0 (39.6)
	Extracts	0.9	0.91	50.6	1.5	0 (44.4)	1.6	0 (39.1)
	Ash	0.6	0.2	82.1	0.1	0 (95.2)	0.3	0 (81.8)
	Solid recovery (SRY, %)	–	50.2	–	68.01	–	70.71	–
WW + HWE	equivalent cellulose	35.3	50.9	30.6	44.0	34.6 (54.6)	44.8	31.0 (52.1)
	equivalent hemicellulose	11.2	1.6	93.2	1.2	40.5 (95.9)	1.2	38.6 (95.8)
	Klason lignin	21.0	37.1	15.1	44.1	0 (23.5)	44.3	0 (20.5)
	Extracts	18.9	0.63	98.4	0.8	0 (98.5)	0.6	0 (98.8)
	Ash	0.1	0.2	41.2	0.2	0 (34.0)	0.1	0 (65.3)
	Solid recovery (SRY, %)	–	48.1	–	75.69	–	78.30	–

(WW). The separated WW and willow biomass (including bark, WB) were dried at 50 °C in oven for 48 h. Additionally, tap water together with the WB (liquid to solid ratio of 10:1) were applied to prepare the hot water extracted willow biomass (HWE WB) by removing the water-soluble phenol-rich extracts (Table S1) at 80 °C for 30 min. WW, WB and HWE WB were ground under the screener diameter size of 0.7 mm (Wiley mill USA/motor: Strömberg Oy). The ground samples were stored at −20 °C before further experimental use. Sulfuric acid (purity of 98%), acetone (99.9%), cellulase enzyme blend (206 FPU/ml), furfural (99%), HMF (99%), acetic acid (99%), butyric acid (99%), citric acid (99%), ethanol (94%), butanol (99.5%), activated carbon (4–14 mesh), DMSO-d_6, pyridine-*d5* and all the nutritional medium components were supplied from Sigma Aldrich, Finland Oy. Calcium hydroxide (95%) was supplied by Acros Organics (Fisher Scientific, USA).

2.1. Steam explosion pre-treatment

Steam explosion (SE) was simulated in a pilot reactor system (constructed by Aalto University Workshop, Finland) consisting of a 10 L reactor vessel heated by an oil-jacket and connected to a 10 L steam generator and a 10 L collection tank. The reactor system was controlled by the *eLabs* program. Prior to SE, the milled biomass (Fig. 1) was impregnated in 0.5 wt% H_2SO_4 solution overnight, with a liquor-to-solid (L:S) ratio of 10:1, and subsequently dewatered by centrifugation to a dry-matter content (DMC) of approximately 40% before loading to the reactor vessel. The biomass was heated to 205 °C (*ca.* 16.3 bar gauge) by the combination of oil-jacket heating and steam (fed from the steam generator to a L:S of 4:1) and held for 5 min before releasing pressure to the collection tank, resulting in a P-factor of about 2000 (see 2.6 Calculations). Due to hardware limitation, the pressure relief (5–8 s to drop from 16.3 to 8 bar, 15–20 s to 3 bar and about 30–45 s to reach atmospheric pressure, respectively) was slower than typical steam exploder, in which the pressure drop to atmospheric pressure happens in seconds. However, the pressure relief in the reactor system should induce adequate temperature and pressure stress to the biomass cell wall, resulting in higher accessible structure for subsequent treatments. The SE-biomass was washed intensively with deionized water until neutral pH, dewatered by centrifugation and dried at 50 °C for 48 h. The hemicellulose-rich hydrolysates fractions obtained from this stage were stored for future reference but not analysed and investigated within the scope of this paper.

2.2. Enzymatic hydrolysis and detoxification

SE-treated samples (10 and 15% w/v) were loaded with 20 FPU/g equivalent cellulose (Cellic CTec2, Sigma-Aldrich, Finland Oy) and 100 mL 50 mM acetate buffer (pH 5) in 250 mL Erlenmeyer flasks. Enzymatic hydrolysis (EH) was conducted by shaking the solution in an incubator (250 rpm) at 50 °C for 72 h. The final hydrolysates were filtrated through Por. 3 crucibles to separate the solid residues from the fermentable sugars. The obtained solids were washed with distilled water for three times and then freeze-dried before lignin purification. The filtered hydrolysates were detoxified by introducing 5% (w/v) activated charcoal (Hydrodarco B, CABOT, Norit American, Inc., Marshall, USA) into the incubator (200 rpm) at the temperature of 28 °C for 1 h. The detoxified hydrolysates were centrifuged to capture the pure fermentable sugars for ABE fermentation. Two independent tests were performed. Each test compromises triplicate trials. The blank assays for enzymes-only in enzymatic hydrolysis were performed to subtract its associated sugars (Table S2).

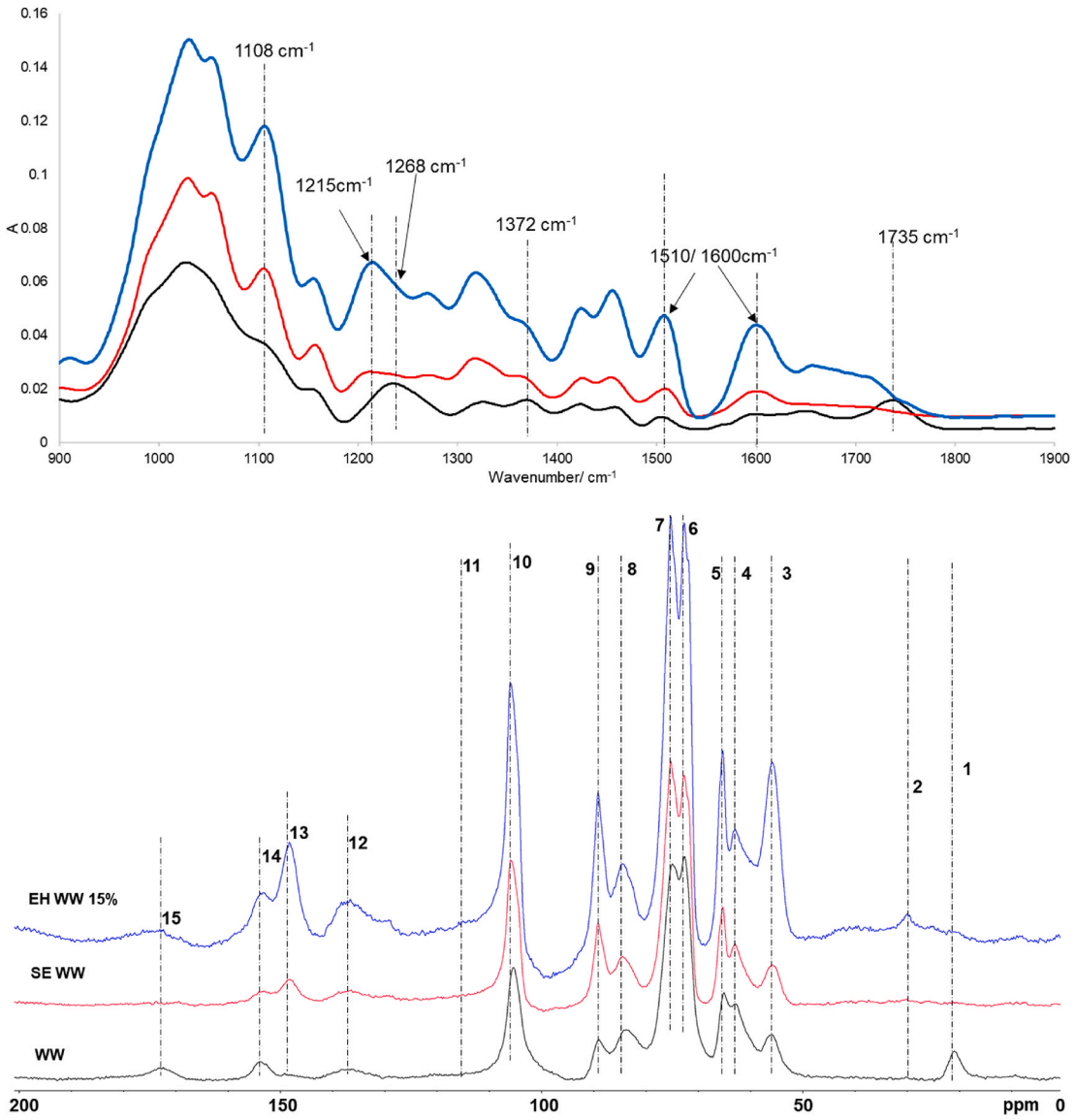

Fig. 2. Infrared spectrum (top) and solid-state ^{13}C CP/MAS NMR spectrum (bottom) of WW (black); SE WW (red); EH WW (blue). For abbreviations: WW = Willow wood; SE WW = steam explosion treated willow wood; EH WW = enzymatic hydrolysis treated willow wood. (For interpretation of the references to colour in this figure legend, the reader is referred to the Web version of this article.)

2.3. Microorganism and fermentation

Pre-culturing of C. *acetobutylicum* NRRL B-527 cells (Agricultural research services culture collection, USA) were anaerobically conducted by inoculating 2.5% v/v spore suspension together with 100 mL sterilized reinforced clostridial medium (RCM) inside the 125 mL screw-capped glass bottles. The recipe (in g/L) of RCM media (pH 6.8) contains (Pratto et al., 2020): meat extract (10); bacto peptone (5); yeast extract (3); starch (1); NaCl (5); sodium acetate (3); L-cysteine (0.5); D-glucose (30). The *Clostridal* spores were activated by heat shock at 80 °C water bath (10 min) before germinating cells inside the ice bath (5 min). The pre-culture was cultivated at 37 °C for 20 h. The production medium (P2) was prepared (in g/L) as follows (Pratto et al., 2020): $MnSO_4.H_2O$ (0.01); $MgSO_4.7H_2O$ (0.2); NaCl (0.01); ammonium acetate (2.2); K_2HPO_4 (0.5); *p*-amino benzoic acid (0.1); thiamine hydrochloride (0.1); biotin (0.01); $FeSO_4.\ 7H_2O$ (0.01); KH_2PO_4 (0.5). The ABE fermentation was initiated by inoculating 5% v/v preculture into 125 mL screw-capped anaerobic glass bottles containing 75 mL willow hydrolysate and 20 mL P2 medium at 37 °C. The fermentation was carried out for 96 h and samples were taken every 24 h to monitor the production of ABE solvents. Fermentation batches were conducted in two independent tests to ensure reproducibility of results, each comprises triplicate samples.

2.4. Lignin purification

The obtained solids after SE and EH were first solubilized (1:50 w/v) using 0.25 M NaOH along with a magnetic stirrer (150 rpm) at room temperature for 10 min. Strong alkaline conditions (pH 13.5) were maintained to facilitate lignin dissolution. 10% Acetic acid (1:5 v/v) with a magnetic stirrer in the Büchner flask preserved an acidic environment (pH 4.1) before filtering the alkali solution. Distilled water was introduced to facilitate the lignin precipitation on ice bath followed by centrifugation at 8000 rpm to capture the precipitated lignin. The captured lignin was then lyophilized for further studies.

2.5. Analytics

Fig. S1 summarizes the analytical techniques applied in this study. The investigated samples were hydrolysed according to NREL/TP-510-

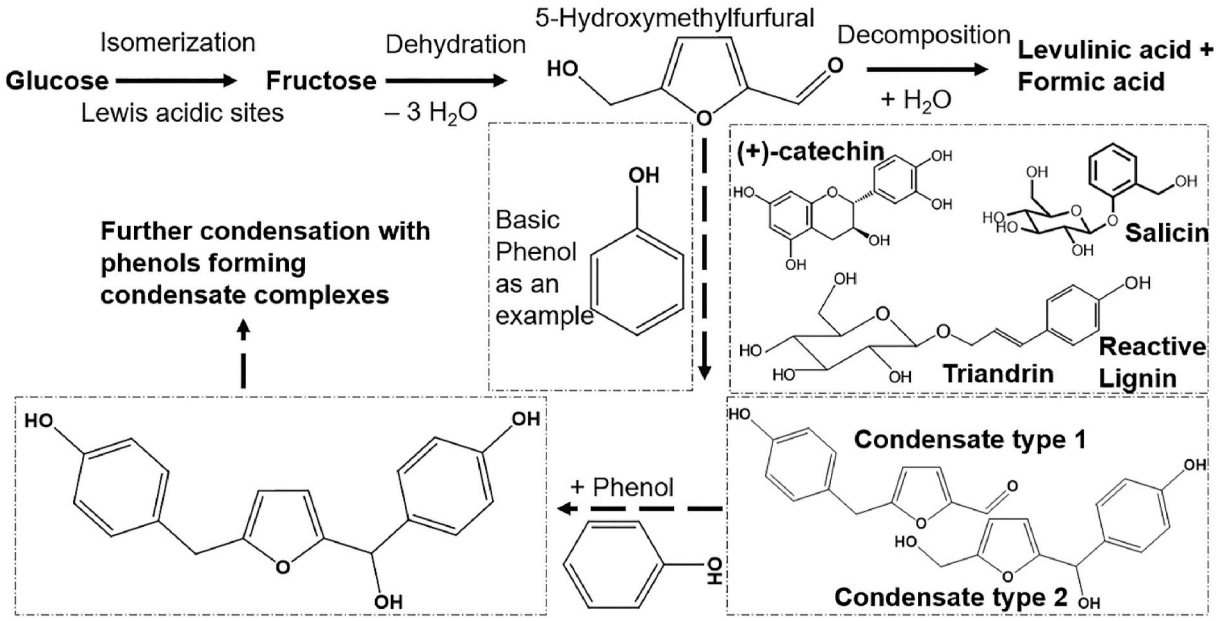

Fig. 3. Proposed phenol aldehyde condensation mechanism during the steam explosion in presence of acid catalyst. Formation of HMF and possible phenol-aldehyde condensations taking place via the aldehyde (condensate type 2) or the methylol group (condensate type 1).

Table 2
Effect of biomass loading (10% w/v; 15% w/v) on Enzymatic Hydrolysis (EH) using four willow-based biomasses. Equation monosaccharide yield = sum hydrolysable sugars (g)/initial biomass (g) (3). For abbreviations see Fig. 1. For standard deviations, see Table S7.

unit g/L	WW		WB		HWEWB		WW + HWE	
	10% w/v	15% w/v	10% w/v	15% w/v	10% w/v	15% w/v	10% w/v	15% w/v
Glucose	41.7	58.0	19.9	30.3	25.8	37.3	18.7	25.9
Xylose	0.5	0.7	0.2	0.4	0.4	0.6	0.4	0.6
Mannose	0.0	0.0	0.0	0.1	0.1	0.1	0.1	0.1
Hydrolysable sugars (sum)	42.2	58.7	20.1	30.8	26.3	37.9	19.2	26.6
HMF	0.01	0.01	0.003	0.004	0.004	0.004	0.005	0.005
Furfural	0.003	0.003	0.001	0.001	0.001	0.001	0.001	0.002
Acetic acid	2.94	2.98	2.61	2.98	3.01	3.08	2.40	2.99
sum inhibitors (sum)	2.96	3.00	2.61	2.99	3.01	3.09	2.41	3.00
Monosaccharide yield %	42.3	39.2	20.0	20.3	26.0	25.2	19.0	17.7

42618 [Sluiter et al., 2010]. Monosaccharides (i.e. glucose, xylose, mannose, arabinose, rhamnose and galactose) were quantified using the high-performance anion-exchange chromatography with pulse amperometric detection (HPAEC-PAD) along with a CarboPac PA 20 column. Pure water with flow rate of 0.38 mL/min was used as the mobile phase at the Dionex ICS-3000 system under room temperature (Dou et al., 2018b).

High-performance Liquid Chromatography (HPLC, Dionex Ultimate 3000) was used to determine dehydration products (HMF and furfural) and acids (acetic acid and butyric acid) using ultraviolet (UV) detector at 280 nm and 210 nm, respectively. Butanol was quantified using refractive index (RI) detector. The column used was Phenomenex Rezex ROA-Organic Acid H^+ (8 μm, 300 × 7.8 mm, Thermo Scientific, USA) and 0.0025 M H_2SO_4 was used as the eluent at a flow rate of 0.5 mL/min at 55 °C. The injection volume was 10 μL and the total run time was 60 min (Pratto et al., 2020).

Produced solvents (acetone and ethanol) were quantified by gas chromatography (GC, Agilent Technologies 7890 B) with flame ionization detection (FID) using an AB-INNOWAX capillary column (30 m × 0.32 mm, 1 μm film). The temperature was maintained at 200 and 250 °C for the injector and FID, respectively (Pratto et al., 2020).

Solution-state nuclear magnetic resonance (NMR) spectra of the purified lignin were acquired on an AVANCE III 400 spectrometer (Bruker, Billerica USA) equipped with 5 mm BBFO probe. Two-dimensional heteronuclear single quantum coherence (HSQC) spectra were acquired at 22 °C with spectral widths of 12.8 ppm and 165 ppm for ^{1}H and ^{13}C, respectively. DMSO-d_6/pyridine-$d5$ (4:1) solvent (Dou et al., 2018a) was used as an internal reference (δC/δH, 39.5/2.49 ppm). A relaxation delay of 2s, d24 delay of 0.89 ms and 1K data points were applied for HSQC (hsqcetgpsisp.2 pulse sequence from the Bruker Library). Solid state ^{13}C CPMAS NMR spectra were measured using Bruker Avance III spectrometer operating at 500 MHz for protons using a double resonance CPMAS probehead. Samples were packed into 4 mm o.d. ZrO_2 rotors and plugged with KEL-F endcaps and spun at spinning frequency of 8 kHz. The length of the contact time for cross polarization was 1 ms and a variable amplitude cross polarization ramped from 70% to a maximum amplitude during the used contact time. During the acquisition period the protons were decoupled using SPINAL-64 decoupling and the length of the acquisition was 27 ms. At least 3000 scans were collected with a 5 s relaxation delay and the spectra were externally referenced to adamantane (Dou et al., 2021a). TopSpin 4.0 was adopted to analyse all NMR spectra.

High performance size-exclusion chromatography (HP-SEC) system was applied through columns (PSS MCX 5 μm 300 mm × 8 mm, 100, 500, and 1000 Å) using 0.1M NaOH as the eluent at 30 °C. The samples were first dissolved in 0.1 M NaOH before filtering through a 0.45 μm membrane prior to the analysis. Mn (number-averaged molecular weight), Mw (weight-averaged molecular weight) and polydispersity

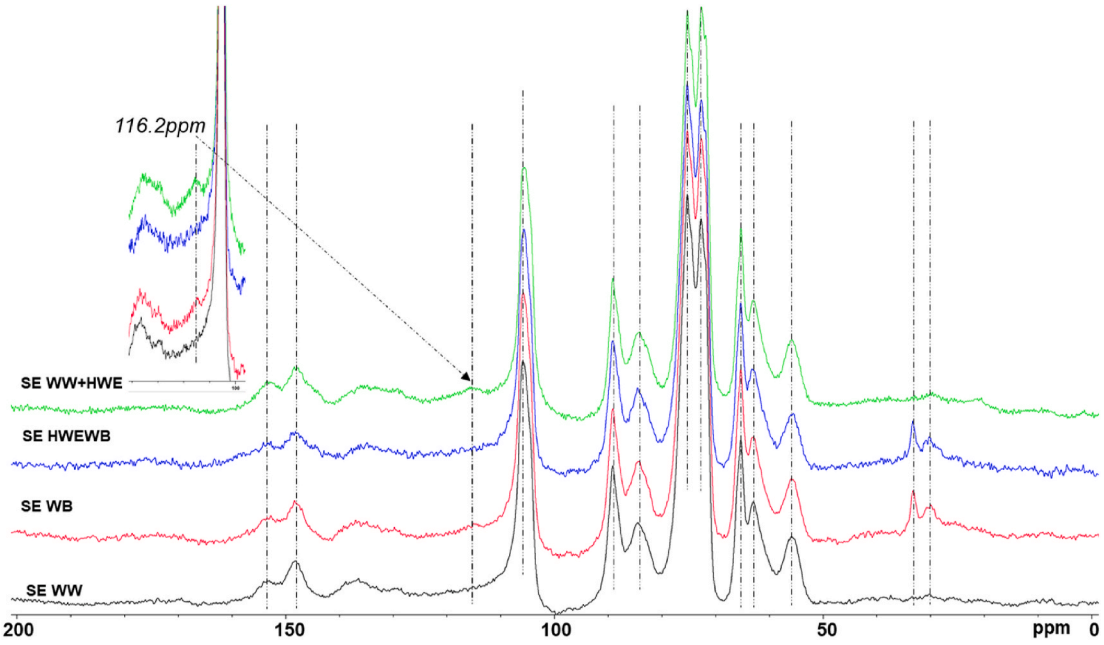

Fig. 4. Solid-state ^{13}C CP/MAS spectra of solid residues after steam explosion (SE): a) SE WW; b) SE WB; c) SE HWEWB; d) SE WW + HWE. Abbreviations: SE WW = steam explosion treated WW; SE WB = steam explosion treated WB; SE HWEWB = steam explosion treated HWEWB; SE WW + HWE = steam explosion treated WW + HWE. The included screenshot is magnified for 50x.

Table 3
Structural characteristics of purified lignins from the recovered WW; WB; HWEWB; WW + HWE after the enzymatic hydrolysis (15% w/v) in comparison to the WW EL (Dou et al., 2018a) obtained by integration of ^{1}H–^{13}C correlation contours in the corresponding HSQC Spectra (Fig. 5).

	WW EL	EH WW	EH WB	EH HWEWB	EH WW + HWE
Lignin interunit linkages (%)[a]					
β-O-4′ aryl ethers (A'/A)	89	51	44	48	58
Phenylcoumaran (B)	3	17	9	13	6
Resinols (C)	7	32	47	40	36
Lignin aromatic units[b]					
G (%)	34	16	10	15	12
S (%)	66	84	90	85	88
S/G ratio	1.9	5.3	8.8	5.7	7.4

[a] Percentage of total volume of A, B, and C signals (calculated from the α-C/H correlations).
[b] Percentage of total volume of G2, G′2, S2/6, and S′2/6 signals.

index (PDI) were measured as described previously (Dou et al., 2021c).

Fourier transform infrared spectroscopy (FT-IR) attenuated total reflection (ATR) (PerkinElmer, UK) was adopted to measure the IR absorption spectra in range of 4000–500 cm^{-1} with an acquisition time of 30 s.

2.6. Calculations

The intensity of the applied steam explosion is expressed as p-factor using an Arrhenius-type expression where t refers to the pre-hydrolysis time (min) and T is the pre-hydrolysis temperature (K). P factor refers to the pre-hydrolysis intensity, and this equation is based on the applied reaction kinetics and activation energy for cleavage of glycosidic bonds (Sixta, 2006).

$$P = \int_{to}^{t} e^{40.48-15106/T} dt \quad (1)$$

3. Results & discussion

This study demonstrates the importance of debarking or water extracts removal for the increase of enzymatic hydrolysis and the subsequent ABE fermentation for willow biomass, as illustrated in Fig. 1. Four types of materials (i.e. WW, WB, HWEWB and WW + HWE of Fig. 1) were comparatively chemically evaluated during the stages of steam explosion pre-treatment, enzymatic hydrolysis and ABE fermentation, the chemical characteristics of the formed phenol-aldehyde condensate are all together discussed in the subsequent sections.

3.1. Effect of steam explosion

Solid recovery yields after steam explosion (approximately 42–50 wt %) shown in Table 1 were low because of the material losses during the steam explosion and the washing. Similar low yields are also reported for spruce bark using the steam explosion pre-treatment (Kemppainen et al., 2012). Steam explosion pre-treatment (205 °C/5 min) at Table 1 resulted in almost complete (93–97 wt%) removal of the hemicelluloses using the sulfuric acid as the catalyst, seen as substantial reduction of the methyl carbon of acetyl groups in hemicellulose by infrared spectroscopy (at 1735 cm^{-1}) (Salim et al., 2021) and ^{13}C CP/MAS NMR spectroscopy (at 21.1 ppm) (Hu et al., 2014) in Fig. 2. Detailed assignments are summarized in Table S3 and Table S4. The relative content of the cellulose and lignin in the recovered solid residues has increased in comparison to the untreated biomass due to the degradation of hemicelluloses. Steam explosion is known to bring easier cellulase accessibility with the enzymatic saccharification by loosening the cell wall structure (Silveira et al., 2015), which facilitates the partial degradation of lignin and cellulose (Sixta, 2006). Approximately 30% of cellulose (or glucose equivalent, Table 1) degraded due to the applied steam explosion (P-factor of 1950–2050). A 23% reduction of glucose has been reported for birch wood at P factor of 1000 (Testova et al., 2011). Moreover, relative changes of the cellulose crystallinity in the samples were approximately assessed by directly comparing the signal intensities of C4 crystalline (i.e. 89.2 ppm) and noncrystalline (i.e. 84.6 ppm) lines although xylan adsorbed on cellulose also contributes to the signal at

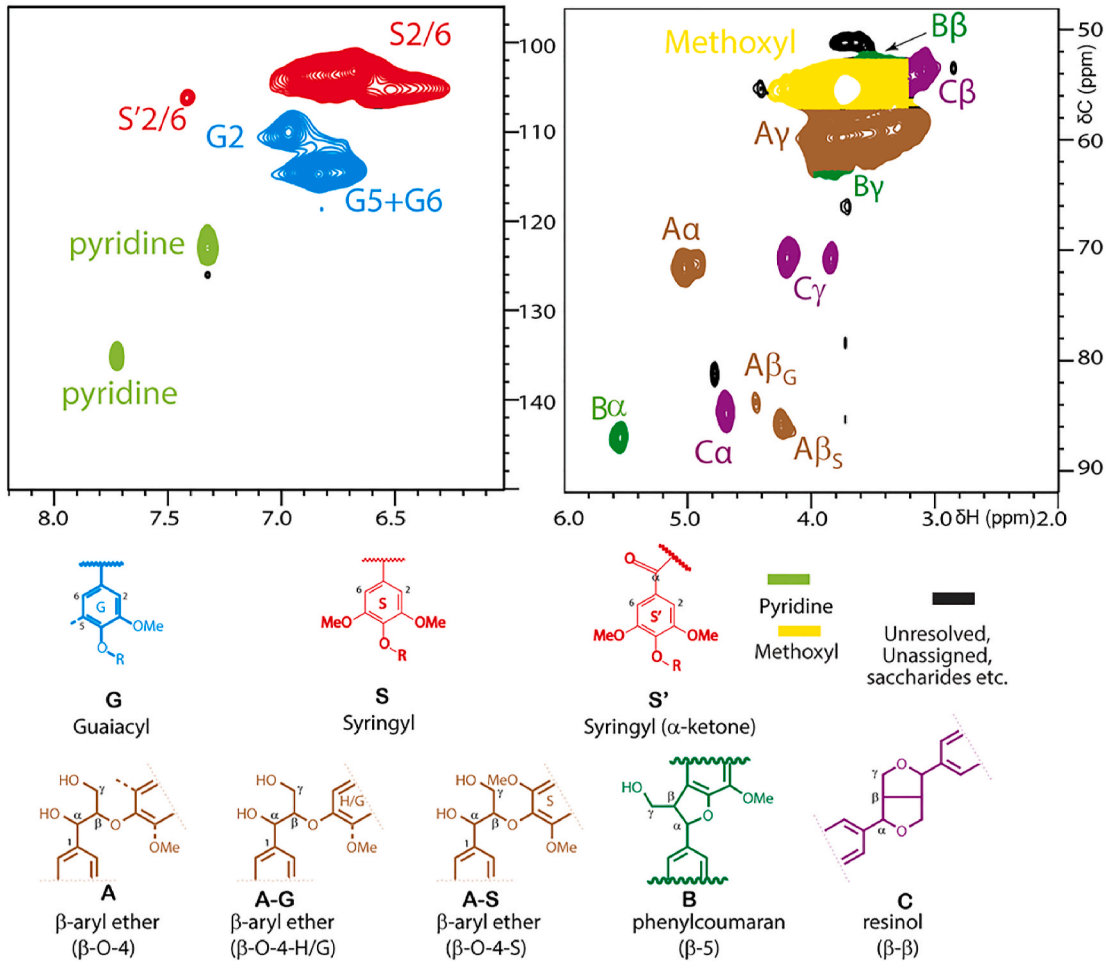

Fig. 5. Aromatic (δC/δH, 96–150/6.0–8.2 ppm) and side-chain (δC/δH, 48–92/2.0–6.0 ppm) regions of 2D HSQC NMR spectra of EH WW Lignin prepared after steam explosion and enzymatic hydrolysis.

84.6 ppm (Larsson et al., 1999) for original samples. The apparent crystallinity of cellulose increased after the steam explosion pre-treatment (Fig. 2 and Table S6), which favors the enzymatic hydrolysis (Hall et al., 2010; Silveira et al., 2015). However, the correlation between the crystallinity index with the pre-hydrolysis rate is beyond the scope of the present study. Additionally, the relative proportion between the integral intensities of cellulose and lignin increased after the SE pre-treatment (Table S6), which indicates that the degradation of cellulose induced by SE pre-treatment was less severe than that of lignin. Moreover, changes in the aromatic region suggest that mostly reactive syringyl-type lignin was solubilized as the methoxyl content depends on the syringyl-to-guaiacyl ratio.

It has been hypothesized that under acidic conditions fructose present in willow Klara water extracts (Table S1) forms hydroxymethylfurfural (HMF) (Maiti et al., 2016) which then spontaneously condenses with phenolic compounds to form a solid precipitate (Dou et al., 2018b; Koch and Pein, 1985), as visualized in Fig. 3. The "Klason Lignin'' content of WW + HWE (Table 1) displayed the minimal reduction after the steam explosion in comparison to the remaining three samples. This suggested that phenolic components (i.e., catechin and triandrin, and other uncharacterized polyphenols and reactive phenol-type lignin) of willow bark (Table S1) that would otherwise dissolve in water condensed under acidic conditions, causing an overestimation of the "Klason lignin" in the recovered residue. Kemppainen et al. (2012) also conducted steam explosion as pre-treatment for ethanol production from spruce bark and they reported a 10 wt% total mass yield increase with the acid-catalysed steam explosion (T 205 °C) in comparison to the same temperature conditions without acid as the catalyst. This supports the hypothesis that the formed condensate was misidentified as "Klason lignin" in the recovered solid residues. The detailed chemical structure of the solid residue is further elucidated in section 3.3. Although the furfural (conversion from xylose) (Choudhary et al., 2012) also contributes to the condensation with phenols that is present at willow bark water extracts, this is not considered in this study as willow bark water extracts (Table S1) don't contain xylose. Further work is required to unveil the formation mechanism by analogous reactions of model compounds and understand the importance of this specific reaction depending on the biomass fraction and its pre-treatment environments.

3.2. Enzymatic hydrolysis

Clear decrease in the relative content of glucose is seen after the enzymatic hydrolysis (EH) in comparison to the steam explosion (SE) treated samples at Table 1. The hydrolysis efficiency of cellulose during the EH treatment followed the order of WW > HWE WB > WB > WW + HWE. This is because of the formed precipitates (Fig. 3) in WB and WW + HWE may play inhibitory role in hindering the enzymatic hydrolysis, as supported by the monosaccharide yield differences in Table 2. Specifically, debarked willow wood (WW) generated approximately twice the monosaccharide amount to that of the phenol extractive containing willow samples (i.e. WB and WW + HWE) irrespective of 10% w/v and 15% w/v loadings. HWE WB produced second highest monosaccharide after enzymatic hydrolysis. This result corroborates the hypothesis of

Table 4
Effect of biomass types on ABE fermentation after 96 h using the detoxified hydrolysate. Standard deviations are displayed at Table S11.

concentration g/L	WW	WB	HWEWB	WW + HWE	WW + HWE (M)[a]
Glc after EH	59.2	25.3	42.7	23.0	23.0
Xyl after EH	0.9	0.4	0.7	0.5	0.5
Glc after detoxification	55.2	23.3	37.0	19.2	19.2
Xyl after detoxification	0.5	0.3	0.6	0.5	0.4
Glc at D0 (day 0)	48.1	22.2	27.5	19.2	28.9
Xyl at D0	0.6	0.2	0.3	0.4	0.5
Glc at D4 (day 4)	7.3	0.0	0.0	0.0	0.1
Xyl at D4	0.4	0.1	0.2	0.2	0.3
sugars consumed	40.9	22.3	27.6	19.3	29.0
Acetic acid	2.8	4.1	3.7	3.2	4.6
Butyric acid	1.6	2.1	1.6	1.7	2.3
Total acids	4.3	6.2	5.4	4.9	6.9
HMF	0.005	0.001	0.001	0.0005	0.001
Acetone[b]	3.4	1.4	2.2	1.0	1.7
Butanol[c]	8.5	3.7	5.5	3.0	5.6
Ethanol[b]	0.8	0.3	0.6	0.3	0.5
ABE	12.7	5.5	8.3	4.3	7.8
Butanol yield (100%)[d]	0.21	0.17	0.20	0.16	0.19
ABE yield (100%)[e]	0.31	0.25	0.30	0.22	0.27

[a] Manually increased the initial (i.e. Day 0) concentration from 19.2 g/L to 28.9 g/L, which was used to justify the negative impact of artificial HWE on ABE fermentation.
[b] Quantified by GC-FID.
[c] Quantified by HPLC.
[d] Equation butanol yield (100%) = produced butanol (g)/sugars consumed (g) (4).
[e] Equation ABE yield (100%) = (produced acetone + butanol + ethanol) (g)/sugars consumed (g) (5).

formation of phenol aldehyde condensate (Fig. 3) in pre-treated solid material of WB and WW + HWE due to presence of phenolic extractives which negatively impacted enzyme binding to pre-treated solid and thereby affecting monosugar yield adversely in phenol extractive containing willow samples, which highlights quintessential role of debarking (or removal of phenolic extracts) from willow biomass prior to pre-treatment and subsequent enzymatic hydrolysis. Interestingly, phenolic compounds were also reported to inhibit cellulase and xylanase activity in sugarcane bagasse (González-Bautista et al., 2017). The inhibition mechanism of phenolic compounds is reported to disrupt microbial cell membranes through the combination of hydrophobic interactions and hydrogen bonding (Sun et al., 2016; Castelli et al., 1999).

Although the 10% w/v showed a relatively higher hydrolysate yield than the 15% w/v ones, additional supplementation of glucose will be required to reach 60 g/L concentration in all experiments. Interestingly, WW achieved the notable yield of 42–58 g/L glucose, which was roughly twice than the reported glucose of the acid hydrolysates from 2-year-old willow wood (Han et al., 2013). Furthermore, the recovered solid precipitate after EH (i.e. 75.69% and 78.30% for 10% w/v and 15% w/v, respectively) remained to be the highest in WW + HWE (Table 1). This again justifies the initial hypothesis that the formation of the proposed phenol-aldehyde condensate complexes contributed to the mass of the recovered solid. Table S8 shows the effect of detoxification on elimination of inhibitors (i.e. HMF and furfural), which favours the *Clostridial* growth during ABE fermentation (Pratto et al., 2020). Additionally, acetic acid is formed from the acidic hydrolysis of the acetyl groups in hemicellulose (Steinbach et al., 2017), which was not affected by the detoxification. Further efforts are underway to investigate the optimal pre-treatment for maximizing the yield of hydrolysable sugars for ABE fermentation from lignocellulosic biomass and the feasibility study without detoxification.

3.3. Characteristics of the precipitates

The detailed chemical structure of the solid precipitates (after steam explosion and enzymatic hydrolysis) and its purified lignin were comparatively investigated by nuclear magnetic resonance (NMR) spectroscopy, infrared spectroscopy, and high-performance size-exclusion chromatography (HP-SEC) to understand the formation of the proposed phenol-aldehyde condensate complexes. Infrared spectrum of the SE WW + HWE in Fig. S2 shows a strong absorption at 1710 cm^{-1} which is the characteristic of the C═O stretch from levulinic acid (Koch and Pein, 1985), as the consecutive product of the formed HMF in Fig. 3. The peak at 1645 cm^{-1} represents the formed furfural structure (i.e. condensate type 1 in Fig. 3), which indicates that the condensation with phenol takes place at least partly via the methylol group of HMF (Fig. 3) and showed the highest intensities (Table S6) in WW + HWE. Solid-state ^{13}C CP/MAS NMR spectrum reveals the characteristic furan signals in 116.2 ppm and 148.2 ppm (van Zandvoort et al., 2015) as depicted in Fig. 4 and Figs. S3–S5. Especially the furan signal at 116.2 ppm (Fig. 4) refers to the CH group of the developed furan structure, not as part of the purified lignin (Fig. S6), which showed a higher intensity (Table S6) in WW + HWE both after steam explosion (Fig. 4) and enzymatic hydrolysis (Fig. S3). The over-expression of furan in the solid residues of WW + HWE and WB was observed and suggests the formation of the furanic phenol-aldehyde condensate. The peaks at 30.1–33.16 ppm (Lopes et al., 2000; Dou et al., 2021d) were tentatively assigned to suberin, which shows the difficulty of the suberin removal. Moreover, the intensity of methoxyl signals in the lignin region (i.e. 56.1 ppm) was more pronounced in solid residues of SE WW and EH WW (Table S6), which indicates a more effective cellulose hydrolysis in WW-derived samples as compared to other samples.

To gain a deeper understanding about the chemical structure of the precipitates formed after SE and EH, dissolution in alkali and acidification were applied to purify the lignin out of the solid residue. All purified lignin fractions were investigated through 2D HSQC NMR spectroscopy and assigned according to the literature (Dou et al., 2018a). The steam explosion pre-treatment induced reductions in the amounts of β-O-4′ aryl ethers as indicated in Table 3, meanwhile this brings an increase in the structures of phenylcoumaran and resinols. S/G increased from lignin isolated enzymatically (EL) (S/G 1.9) to the purified WW EH lignin (S/G 5.3), which justified the hypothesis that the reactive syringyl-type lignin has been solubilized at SE pretreatment. By calculation, 28 wt% solid residues (i.e. 6.71 wt% initial willow wood and 32 wt% Klason Lignin) can be purified as “native lignin’’ from EH WW solid residues, which shows a significant yield difference compared to other EH-treated samples. Moreover, the “native lignin’’ backbone structure of EH WW wasn’t noticeably modified (Fig. 5, Table S9) in comparison to the EL (Dou et al., 2018a) although its molecular weight (Mw) has reduced (Table S10). Similar findings about the effect of steam explosion towards its lignin were also reported for poplar (Wang et al., 2020) and wheat straw (Heikkinen et al., 2014). Moreover, the molecular weight (Mw) and its polydispersity index (PDI) of WW-derived lignin were the highest in comparison to other samples (Table S10), which indicated that the degradation degree of purified EH WW lignin was the lowest (Table S10). Overall, these results point out that EH WW lignin has the potential to be further valorised for producing small-molecular weight chemicals. The HSQC spectra of purified lignin from other SE-treated willow residues are elucidated in Figs. S7–S9.

3.4. Fermentation

As expected, due to higher monosugar quantity, WW produced highest ABE (i.e. 12.7 g/L, Table 4) followed by HWEWB (i.e. 8.3 g/L) while phenolic extractives containing samples (i.e. WB, and WW + HWE) produced 5.5 and 4.3 g/L of ABE, respectively (Fig. 6b, Table 4). Butanol production also followed similar trend where WW generated highest amount 8.5 g/L of butanol, followed by HWEWB (5.6 g/L), WB

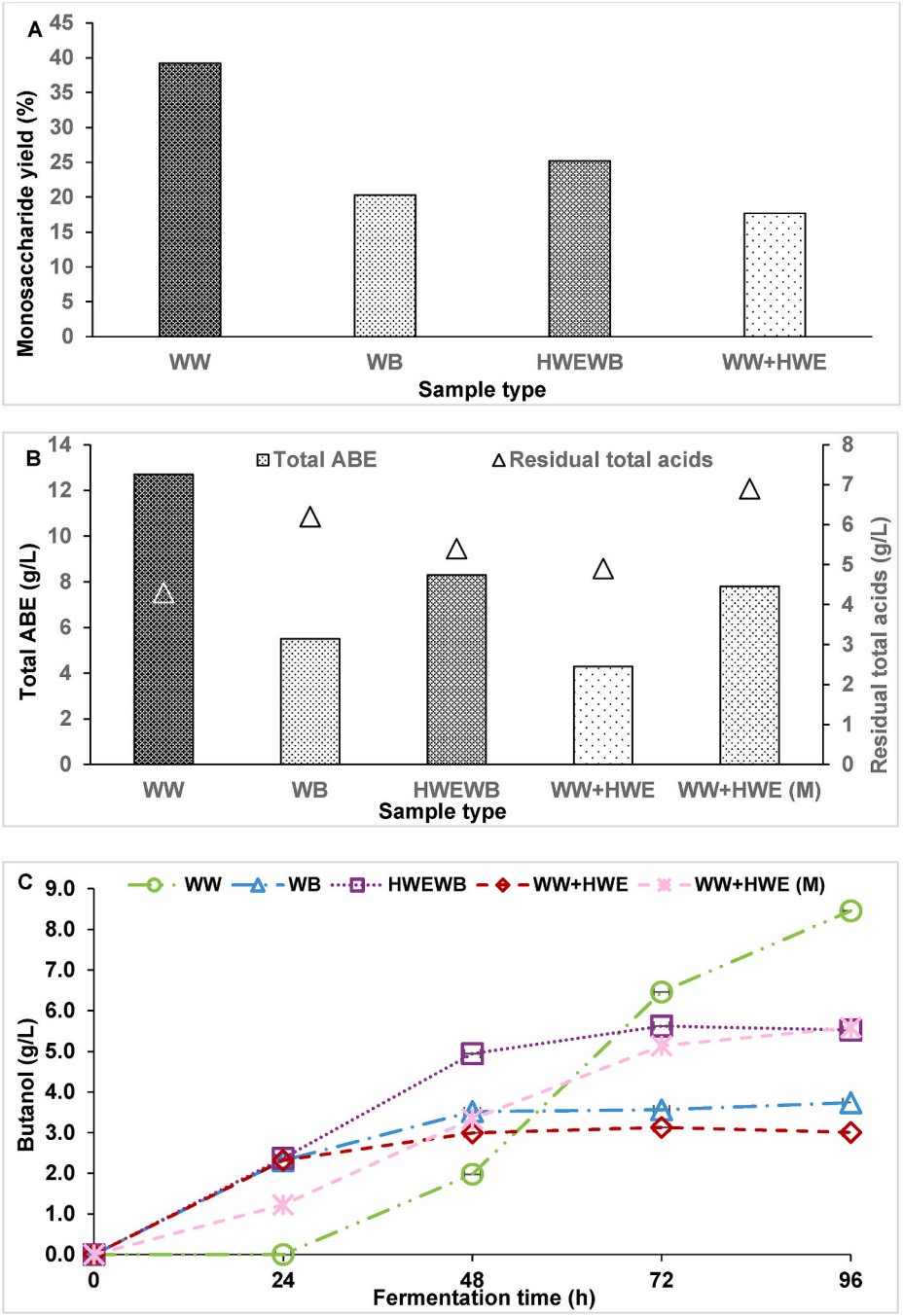

Fig. 6. (A) Effect of enzymatic hydrolysis on monosugar yield in different willow samples (15% w/v) after 72 h; (B) Effect on ABE solvents and residual total acids in different willow samples after 96 h of ABE fermentation; (C) Effect on butanol concentration in different willow samples after 96 h of ABE fermentation.

(3.7 g/L) and WW + HWE (3 g/L) (Fig. 6c). Lower quantities of residual total acids in ABE fermentation medium reflected their higher reassimilation in *Clostridial* cells and therefore their effective conversion in ABE solvents (Chandgude et al., 2021; Pang et al., 2016). Residual amount of total acids also reflected beneficial impact of phenol extractives removal where WW exhibited least amount of residual acid of 4.3 g/L (Fig. 6b, Table 4). High quantity of residual total acids in WB and WW + HWE (M) batch (i.e. 6.9 and 6.2 g/L, respectively) demonstrated the detrimental effect of phenolics on acid reassimilation in *Clostridial* cells. This finding is consistent with that of Cho et al. (2009), who reported high amount of residual acids in presence of phenolic inhibitors in ABE fermentation broth because of their inhibitory effect on acetyl-CoA to butyryl-CoA step in ABE fermentation pathway. Overall, the yields of butanol and ABE declined progressively from WW to HWEWB and WB, and WW + HWE, indicating that the presence of bark (or water extracts) contains inhibitory compounds that are detrimental to the growth of fermentation microorganisms.

Detoxification and ABE fermentation medium preparation have diluted the initial glucose concentration progressively from 59.2 to 55.2 and 48.1 g/L. Although the initial glucose concentration (i.e. 19.2–28.9 g/L) of bark or water extracts containing samples (i.e. WB, HWE WB and WW + HWE) couldn't meet the minimum sugar levels (>40 g/L) (Ibrahim et al., 2015) in the production of *clostridial* ABE fermentation, surprisingly the cells were able to convert the hydrolysable sugars into ABE. Moreover, WW-derived hydrolysates showed slower fermentation growth at the first 24 h (refers to acid-producing period) in comparison

Table 5
Comparison of performance indicators of ABE fermentation with different willow species of its wooden section.

Willow sp. (year-old)	Bacterial Strain	Pre-treatment (T °C) & secondary hydrolysis	Operation mode, carbon source, duration (h)	ABE (g/L)	Butanol (g/L)	Butanol yield (g/g)	ABE yield (g/g)	Reference
Salix schwerinii E. Wolf (6)	*Clostridium acetobutylicum* DSM 1731	Dilute Acid (0.05% (w/v) H_2SO_4) hydrolysis (170 or 200) & Enzymatic hydrolysis	Batch, prehydrolysate liquid + barley grain starch, 144	10.1	6.3	0.22	0.35	Kuittinen et al. (2018)
Salix caprea (2)	*Clostridium beijerinckii* NCIMB 8052	Dilute Acid (4% (w/v) H_2SO_4) hydrolysis (105) (primary and secondary)	Batch, willow hydrolysate, 96	9.4	4.5	0.12	0.25	Han et al. (2013)
Salix schwerinii (6)	*Clostridium acetobutylicum* DSM 1731	Dilute acid (0.1% (w/v) H_2SO_4) hydrolysis (200)	Batch, hemicellulosic hydrolysate + barley grain slurry, 120	10.6	6.7	0.22	0.35	Yang et al. (2017)
Salix schwerinii (6)	*Clostridium acetobutylicum* DSM 1731	Dilute acid (0.1% (w/v) H_2SO_4) hydrolysis (200) & Enzymatic hydrolysis	Batch, *cellulosic hydrolysate* + barley grain slurry, 120	12.4	8.1	0.21	0.33	Yang et al. (2017)
Willow hybrid *Klara* (2)	*Clostridium acetobutylicum* NRRL B-527	Steam explosion with dilute acid (0.5% (w/v) H_2SO_4) (205) & Enzymatic hydrolysis	Batch, cellulosic hydrolysate, 96	12.7	8.5	0.21	0.31	Present study

to others at Fig. 6 and Fig. S10. Thus, the uncharacterized compounds present at willow bark (or its water extracts) were suspected to show positive effects on cellular metabolism for facilitating the ABE fermentation during the first 24 h. On the other hand, WW + HWE (M) showed the increase of phenolic inhibitors brings diverse detrimental effects on its growth within the first 24 h (Table 4) despite its fermentable sugar concentrations were also raised. However, WW + HWE (M) achieved similar production efficiency (i.e. yields of BtOH and ABE) with HWE WB after 96 h fermentation.

WW achieved the highest yields of ABE and butanol compared to the remaining willow samples after 96 h of ABE fermentation. 8.5 and 9.2 g/L of butanol was produced in willow wood batch after 96 and 144 h of ABE fermentation (Table 5), respectively, which is approximately twice the amount of butanol produced from willow wood using acid hydrolysis as the pre-treatment (Han et al., 2013). Table 5 also summarizes comparison of present study with previous investigations conducted with willow species (wood section) in ABE fermentation. The present study achieved highest concentration of ABE solvents compared to previous studies. It also exhibited comparable ABE and butanol yield with the study (Yang et al., 2017) where cellulosic hydrolysate was supplemented with additional carbon source (i.e. barley grain slurry). The effectiveness of debarking and removal of phenolic extractives from willow is evident in the ABE and butanol yields attained in this investigation. Another independent batch study result shown in Table S12 and Fig. S11 verified the stability and reproducibility of the fermentation efficiency. Hence, debarking/hot water extraction of phenolics from willow biomass is proposed as a mean to manipulate outcome of its pre-treatment and subsequent enzymatic hydrolysis and thereby positively impacting ABE fermentation yields. The biobutanol yield doubled in WW batch compared to non-debarked (WB) and phenolic extractives containing batch (WW + HWE), which also resulted in an improved overall ABE solvents yield. Hence the prior removal of phenolic extractives through debarking or hot water extraction is suggested here as an effective tool to eliminate the formation of phenol-aldehyde precipitate during steam explosion, thereby improving yields of enzymatic hydrolysis and its subsequent ABE fermentation. This also allows to utilize the underappreciated willow bark as a potential source of valuable pharmaceutical chemicals (Kesari et al., 2020) and functional materials (Dou et al., 2021c). Advanced bioprocess operation such as continuous operation in packed bed reactor with simultaneous product recovery will be conducted in the future to increase the yields and productivities of ABE fermentation from willow wood.

4. Conclusions

This is the first time that an efficient strategy of prior removal of phenolic extractives via debarking or water extraction from willow is demonstrated, which can not only enhance the efficiency of enzymatic hydrolysis but also increases subsequent ABE fermentation. The hypothesis about formation of phenol-aldehyde precipitate which can hinder the enzymatic hydrolysis has been justified. The formation of this solid precipitate of the hydroxymethylfurfural is a valuable finding as it spontaneously condenses with phenolics under acidic environments. This reminds that similar transformations may occur e.g. during steam explosion of any other lignocellulose-derived biomaterials as their bark also contain phenolic extractives.

CRediT authorship contribution statement

Jinze Dou: Conceptualization, Methodology, Validation, Formal analysis, Investigation, Resources, Funding acquisition, Data curation, Supervision, Project administration, Writing – original draft, Writing – review & editing. **Vijaya Chandgude:** Methodology, Validation, Formal analysis, Investigation, Data curation, Supervision, Writing – original draft (only part of 3.4. Fermentation), Writing – review & editing. **Tapani Vuorinen:** Conceptualization, Investigation, Resources, Writing – review & editing. **Sandip Bankar:** Investigation, Resources, Funding acquisition, Writing – review & editing. **Sami Hietala:** Investigation, Writing – review & editing. **Huy Quang Lê:** Investigation, Writing – review & editing.

Declaration of competing interest

The authors declare that they have no known competing financial interests or personal relationships that could have appeared to influence the work reported in this paper.

Acknowledgements

The authors would like to thank Pitkänen Leena, Hatakka Rita and Linnekoski Juha for their skilful assistance in HP-SEC, HPAEC-PAD and GC-FID measurements. This work made use of the Aalto University NMR premises. This work was a part of the Academy of Finland's Flagship Programme under Projects No. 318890 and 318891 (Competence Center for Materials Bioeconomy, FinnCERES).

Appendix A. Supplementary data

Supplementary data to this article can be found online at https://doi.org/10.1016/j.jclepro.2021.129432.

References

Bankar, S.B., Survase, S.A., Ojamo, H., Granström, T., 2013. Biobutanol: the outlook of an academic and industrialist. RSC Adv. 3, 24734–24757. https://doi.org/10.1039/c3ra43011a.

Birgen, C., Dürre, P., Preisig, H.A., Wentzel, A., 2019. Butanol production from lignocellulosic biomass: revisiting fermentation performance indicators with exploratory data analysis. Biotechnol. Biofuels 12, 167. https://doi.org/10.1186/s13068-019-1508-6.

Castelli, F., Uccella, N., Trombetta, D., Saija, A., 1999. Differences between coumaric and cinnamic acids in membrane permeation as evidenced by time-dependent calorimetry. J. Agric. Food Chem. 47, 991–995. https://doi.org/10.1021/jf980518a.

Chandgude, V., Välisalmi, T., Linnekoski, J., Granström, T., Pratto, B., Eerikäinen, T., Jurgens, G., Bankar, S., 2021. Reducing agents assisted fed-batch fermentation to enhance ABE yields. Energy Convers. Manag. 227, 113627. https://doi.org/10.1016/j.enconman.2020.113627.

Cho, D.H., Lee, Y.J., Um, Y., Sang, B., Kim, Y.H., 2009. Detoxification of model phenolic compounds in lignocellulosic hydrolysates with peroxidase for butanol production from *Clostridium beijerinckii*. Appl. Microbiol. Biotechnol. 83, 1035–1043. https://doi.org/10.1007/s00253-009-1925-8.

Choudhary, V., Sandler, S.I., Vlachos, D.G., 2012. Conversion of xylose to furfural using Lewis and Brønsted acid catalysts in aqueous media. ACS Catal. 2, 2022–2028. https://doi.org/10.1021/cs300265d.

da Silva Trindade, W.R., dos Santos, R.G., 2017. Review on the characteristics of butanol, its production and use as fuel in internal combustion engines. Renew. Sustain. Energy Rev. 69, 642–651. https://doi.org/10.1016/j.rser.2016.11.213.

Dou, J., Galvis, L., Holopainen-Mantila, U., Reza, M., Tamminen, T., Vuorinen, T., 2016. Morphology and overall chemical characterization of willow (*Salix* sp.) inner bark and wood: toward controlled deconstruction of willow biomass. ACS Sustain. Chem. Eng. 4, 3871–3876. https://doi.org/10.1021/acssuschemeng.6b00641.

Dou, J., Kim, H., Li, Y., Padmakshan, D., Yue, F., Ralph, J., Vuorinen, T., 2018a. Structural characterization of lignins from willow bark and wood. J. Agric. Food Chem. 66, 7294–7300. https://doi.org/10.1021/acs.jafc.8b02014.

Dou, J., Xu, W., Koivisto, J.J., Mobley, J.K., Padmakshan, D., Kögler, M., Xu, C., Willför, S., Ralph, J., Vuorinen, T., 2018b. Characteristics of hot water extracts from the bark of cultivated willow (*Salix* sp.). ACS Sustain. Chem. Eng. 6, 5566–5573. https://doi.org/10.1021/acssuschemeng.8b00498.

Dou, J., Karakoç, A., Johansson, L., Hietala, S., Evtyugin, D., Vuorinen, T., 2021a. Mild alkaline separation of fiber bundles from eucalyptus bark and their composites with cellulose acetate butyrate. Ind. Crop. Prod. 165, 113436. https://doi.org/10.1016/j.indcrop.2021.113436.

Dou, J., Heinonen, J., Vuorinen, T., Xu, C., Sainio, T., 2021b. Chromatographic recovery and purification of natural phytochemicals from underappreciated willow bark water extracts. Separ. Purif. Technol. 261, 118247. https://doi.org/10.1016/j.seppur.2020.118247.

Dou, J., Vuorinen, T., Koivula, H., Forsman, N., Sipponen, M., Hietala, S., 2021c. Self-standing lignin-containing willow bark nanocellulose films for oxygen blocking and UV Shielding. ACS Appl. Nano Mater. 4, 2921–2929. https://doi.org/10.1021/acsanm.1c00071.

Dou, J., Evtuguin, D.V., Vuorinen, T., 2021d. Structural elucidation of suberin from the bark of cultivated willow (*Salix* sp.). J. Agric. Food Chem. https://doi.org/10.1021/acs.jafc.1c04112.

Eriksson, T., Börjesson, J., Tjerneld, F., 2002. Mechanism of surfactant effect in enzymatic hydrolysis of lignocellulose. Enzym. Microb. Technol. 31, 353–364. https://doi.org/10.1016/S0141-0229(02)00134-5.

French, A.D., 2017. Glucose, not cellobiose, is the repeating unit of cellulose and why that is important. Cellulose 24, 4605–4609. https://doi.org/10.1007/s10570-017-1450-3.

González-Bautista, E., Santana-Morales, J.C., Ríos-Fránquez, F.J., Poggi-Varaldo, H.M., Ramos-Valdivia, A.C., Cristiani-Urbina, E., Ponce-Noyola, T., 2017. Phenolic compounds inhibit cellulase and xylanase activities of *Cellulomonas flavigena* PR-22 during saccharification of sugarcane bagasse. Fuel 196, 32–35. https://doi.org/10.1016/j.fuel.2017.01.080.

Hall, M., Bansal, P., Lee, J.H., Realff, M.J., Bommarius, A.S., 2010. Cellulose crystallinity – a key predictor of the enzymatic hydrolysis rate. FEBS J. 277, 1571–1582. https://doi.org/10.1111/j.1742-4658.2010.07585.x.

Han, S.H., Cho, D.H., Kim, Y.H., Shin, S.J., 2013. Biobutanol production from 2-year-old willow biomass by acid hydrolysis and acetone-butanol-ethanol fermentation. Energy 61, 13–17. https://doi.org/10.1016/j.energy.2013.04.069.

Heikkinen, H., Elder, T., Maaheimo, H., Rovio, S., Rahikainen, J., Kruus, K., Tamminen, T., 2014. Impact of steam explosion on the wheat straw lignin structure studied by solution-state nuclear magnetic resonance and density functional methods. J. Agric. Food Chem. 62, 10437–10444. https://doi.org/10.1021/jf504622j.

Hu, L., Luo, Y., Cai, B., Li, J., Tong, D., Hu, C., 2014. The degradation of the lignin in *Phyllostachys heterocycla* cv. *pubescens* in an ethanol solvothermal system. Green Chem. 16, 3107–3116. https://doi.org/10.1039/c3gc42489h.

Hytönen, J., Saarsalmi, A., 2009. Long-term biomass production and nutrient uptake of birch, alder and willow plantations on cut-away peatland. Biomass Bioenergy 33, 1197–1211. https://doi.org/10.1016/j.biombioe.2009.05.014.

Ibrahim, M.F., Abd-Aziz, S., Yusoff, M.E.M., Phang, L.Y., Hassan, M.A., 2015. Simultaneous enzymatic saccharification and ABE fermentation using pretreated oil palm empty fruit bunch as substrate to produce butanol and hydrogen as biofuel. Renew. Energy 77, 447–455. https://doi.org/10.1016/j.renene.2014.12.047.

Isikgor, F.H., Becer, C.R., 2015. Lignocellulosic biomass: a sustainable platform for the production of bio-based chemicals and polymers. Polym. Chem. 6, 4497–4559. https://doi.org/10.1039/C5PY00263J.

Jørgensen, H., Kristensen, J.B., Felby, C., 2007. Enzymatic conversion of lignocellulose into fermentable sugars: challenges and opportunities. Biofuels, Bioprod. Biorefin. 1, 119–134. https://doi.org/10.1002/bbb.4.

Kemppainen, K., Inkinen, J., Uusitalo, J., Nakari-Setälä, T., Siika-aho, M., 2012. Hot water extraction and steam explosion as pretreatments for ethanol production from spruce bark. Bioresour. Technol. 117, 131–139. https://doi.org/10.1016/j.biortech.2012.04.080.

Kemppainen, K., Siika-aho, M., Pattathil, S., Giovando, S., Kruus, K., 2014. Spruce bark as an industrial source of condensed tannins and non-cellulosic sugars. Ind. Crop. Prod. 52, 158–168. https://doi.org/10.1016/j.indcrop.2013.10.009.

Kesari, K.K., Dhasmana, A., Shandilya, S., Prabhakar, N., Shaukat, A., Dou, J., Rosenholm, J.M., Vuorinen, T., Ruokolainen, J., 2020. Plant-derived natural biomolecule picein attenuates menadione induced oxidative stress on neuroblastoma cell mitochondria. Antioxidants 9, 552. https://doi.org/10.3390/antiox9060552.

Koch, H., Pein, J., 1985. Condensation reactions between phenol, formaldehyde and 5-hydroxymethylfurfural, formed as intermediate in the acid Catalyzed dehydration of starchy products. Polym. Bull. 13, 525–532. https://doi.org/10.1007/BF00263474.

Kuittinen, S., Yang, M., Kaipiainen, E., Villa, A., Keinänen, M., Vepsäläinen, J., Pappinen, A., 2018. Acetone-butanol-ethanol fermentation of non-detoxified dilute acid extracted hemicellulosic hydrolysate from the short-rotation coppice *Salix Schewerinii*. E. Wolf. BioResources 13, 5225–5240.

Larsson, P.T., Hult, E., Wickholm, K., Pettersson, E., Iversen, T., 1999. CP/MAS ^{13}C-NMR spectroscopy applied to structure and interaction studies on cellulose I. Solid State Nucl. Magn. Reson. 15, 31–40. https://doi.org/10.1016/S0926-2040(99)00044-2.

Lindegaard, K.N., Carter, M.M., Mccracken, A., Shield, I.F., Macalpine, W., Hinton Jones, M., Valentine, J., Larsson, S., 2011. Comparative trials of elite Swedish and UK biomass willow varieties 2001–2010. Aspect Appl. Biol. 112, 57–66.

Lopes, M.H., Gil, A.M., Silvestre, A.J.D., Neto, C.P., 2000. Composition of suberin extracted upon gradual alkaline methanolysis of *Quercus suber* L. Cork. J. Agric. Food Chem. 48, 383–391. https://doi.org/10.1021/jf9909398.

Maiti, S., Gallastegui, G., Sarma, S.J., Brar, S.K., Bihan, Y.L., Drogui, P., Buelna, G., Verma, M., 2016. A re-look at the biochemical strategies to enhance butanol production. Biomass Bioenergy 94, 187–200. https://doi.org/10.1016/j.biombioe.2016.09.001.

Nilsson, A., Shabestary, K., Brandão, M., Hudson, E.P., 2020. Environmental impacts and limitations of third-generation biobutanol: life cycle assessment of *n*-butanol produced by genetically engineered cyanobacteria. J. Ind. Ecol. 24, 205–216. https://doi.org/10.1111/jiec.12843.

Pang, Z.W., Lu, W., Zhang, H., Liang, Z.W., Liang, J.J., Du, L.W., Duan, C.J., Feng, J.X., 2016. Butanol production employing fed-batch fermentation by *Clostridium acetobutylicum* GX01 using alkali-pretreated sugarcane bagasse hydrolysed by enzymes from *Thermoascus aurantiacus* QS 7–2-4. Bioresour. Technol. 212, 82–91. https://doi.org/10.1016/j.biortech.2016.04.013.

Pratto, B., Chandgude, V., Júnior, R.S., Cruz, A.J.G., Bankar, S., 2020. Biobutanol production from sugarcane straw: defining optimal biomass loading for improved ABE fermentation. Ind. Crop. Prod. 148, 112265. https://doi.org/10.1016/j.indcrop.2020.112265.

Salim, R.M., Asik, J., Sarjadi, M.S., 2021. Chemical functional groups of extractives, cellulose and lignin extracted from native *Leucaena leucocephala* bark. Wood Sci. Technol. 55, 295–313. https://doi.org/10.1007/s00226-020-01258-2.

Silveira, M.H.L., Morais, A.R.C., Lopes, A.M.D., Olekszyszen, D.N., Bogel-Łukasik, R., Andreaus, J., Ramos, L.P., 2015. Current pretreatment technologies for the development of cellulosic ethanol and biorefineries. ChemSusChem 8, 3366–3390. https://doi.org/10.1002/cssc.201500282.

Sixta, H., 2006. Handbook of pulp, first ed., 1. Wiley-VCH Verlag GmbH & Co.KGaH, Weinheim, Germany.

Sluiter, J.B., Ruiz, R.O., Scarlata, C.J., Sluiter, A.D., Templeton, D.W., 2010. Compositional analysis of lignocellulosic feedstocks. 1. Review and description of methods. J. Agric. Food Chem. 58, 9043–9053. https://doi.org/10.1021/jf1008023.

Steinbach, D., Kruse, A., Sauer, J., 2017. Pretreatment technologies of lignocellulosic biomass in water in view of furfural and 5-hydroxymethylfurfural production - a review. Biomass Convers. Biorefin. 7, 247–274. https://doi.org/10.1007/s13399-017-0243-0.

Sun, S., Huang, Y., Sun, R., Tu, M., 2016. The strong association of condensed phenolic moieties in isolated lignins with their inhibition of enzymatic hydrolysis. Green Chem. 18, 4276–4286. https://doi.org/10.1039/C6GC00685J.

Testova, L., Chong, S., Tenkanen, M., Sixta, H., 2011. Autohydrolysis of birch wood. Holzforschung 65, 535–542. https://doi.org/10.1515/hf.2011.073.

van Zandvoort, I., Koers, E.J., Weingarth, M., Bruijnincx, P.C.A., Baldus, M., Weckhuysen, B.M., 2015. Structural characterization of ^{13}C-enriched humins and alkali-treated ^{13}C humins by 2D solid-state NMR. Green Chem. 17, 4383–4392. https://doi.org/10.1039/c5gc00327j.

Wang, H., Liu, Z., Hui, L., Ma, L., Zheng, X., Li, J., Zhang, Y., 2020. Understanding the structural changes of lignin in poplar following steam explosion pretreatment. Holzforschung 74, 275–285. https://doi.org/10.1515/hf-2019-0087.

Yang, M., Kuittinen, S., Vepsäläinen, J., Zhang, J., Pappinen, A., 2017. Enhanced acetone-butanol-ethanol production from lignocellulosic hydrolysates by using

starchy slurry as supplement. Bioresour. Technol. 243, 126–134. https://doi.org/10.1016/j.biortech.2017.06.021.

Zhang, J., Tuomainen, P., Siika-aho, M., Viikari, L., 2011. Comparison of the synergistic action of two thermostable xylanases from GH families 10 and 11 with thermostable cellulases in lignocellulose hydrolysis. Bioresour. Technol. 102, 9090–9095. https://doi.org/10.1016/j.biortech.2011.06.085.

Zhang, Y., Xia, C., Lu, M., Tu, M., 2018. Effect of overliming and activated carbon detoxification on inhibitors removal and butanol fermentation of poplar prehydrolysates. Biotechnol. Biofuels 11, 178. https://doi.org/10.1186/s13068-018-1182-0.